Journal of Applied Physics

RESEARCH ARTICLE | MAY 08 2025

On the role of strain- and doping-induced disorder in epitaxial $CaCuO_2$ films: Lattice and spin dynamics in light scattering response

E. Stellino ; P. Postorino; S. Sanna; A. Tebano; D. Di Castro

J. Appl. Phys. 137, 185301 (2025)
https://doi.org/10.1063/5.0263552

Journal of Applied Physics ARTICLE pubs.aip.org/aip/jap

On the role of strain- and doping-induced disorder in epitaxial $CaCuO_2$ films: Lattice and spin dynamics in light scattering response

Cite as: J. Appl. Phys. **137**, 185301 (2025); doi: 10.1063/5.0263552
Submitted: 5 February 2025 · Accepted: 21 April 2025 ·
Published Online: 8 May 2025

E. Stellino,[1,a)] P. Postorino,[2] S. Sanna,[3,4] A. Tebano,[3,4] and D. Di Castro[3,4]

AFFILIATIONS

[1]Dipartimento di Scienze di Base e Applicate per l'Ingegneria, Sapienza Università di Roma, Piazzale Aldo Moro 5, 00185 Roma, Italia
[2]Dipartimento di Fisica, Sapienza Università di Roma, Piazzale Aldo Moro 5, 00185 Roma, Italia
[3]Dipartimento di Ingegneria Civile e Ingegneria Informatica, Università di Roma "Tor Vergata", Via del Politecnico 1, 00133 Roma, Italia
[4]CNR-SPIN, Università di Roma "Tor Vergata", Roma, Italia

[a)]**Author to whom correspondence should be addressed:** elena.stellino@uniroma1.it

ABSTRACT

The infinite layer structure of $CaCuO_2$ (CCO) represents a benchmark system for exploring the physics of CuO_2 planes, which play a fundamental role in superconductive behavior at the high critical temperature of cuprates. In this work, we carried out an extensive investigation of the Raman spectrum of epitaxial films of CCO by varying the degree and origin of disorder in the crystal lattice. A stoichiometric film synthesized on a $[LaAlO_3]_{0.3}[Sr_2AlTaO_6]_{0.7}$ substrate served as a reference to account for the nearly ideal crystal behavior, while defective samples were obtained either by intercalating oxygen in excess in the lattice or by growing the CCO film on a La_2CuO_4 substrate with large lattice mismatch. In the low-frequency region of the Raman spectrum, a strong correlation was observed between the degree of disorder of the film and the enhancement of the phononic activity at resonant excitation energies near the charge transfer gap. Conversely, the magnon-pair band, visible in the spectrum at excitation energies well above the charge transfer gap, displayed only subtle differences among the three samples. A systematic analysis as a function of the in-plane polarization angle identified two contributions to the magnon-pair light scattering mechanism: a dominant one with B_{1g} representation and a secondary one with A_{1g} representation, which appeared to be enhanced in the strained film grown on the La_2CuO_4 substrate. Overall, our work provides new insights into the response of CCO epitaxial films to strain- and doping-induced disorders. The results indicate a greater sensitivity of lattice dynamics to defects compared with spin dynamics in light scattering processes, suggesting a decoupling between lattice- and spin-related degrees of freedom.

INTRODUCTION

The discovery of high-temperature superconductivity[1] in cuprates has stimulated extensive research efforts into all materials of this class, including not only superconductors but also undoped insulating crystals. Indeed, superconductivity at a high critical temperature, T_c, emerges near the antiferromagnetic instability when holes or electrons are doped into the insulating parent compounds, such as La_2CuO_4 and Nd_2CuO_4.[2] Consequently, a detailed investigation of the parent compounds can play a fundamental role in understanding the physical mechanisms underlying the superconducting behavior in cuprates.

It is widely accepted that the fundamental physical processes contributing to high-T_c superconductivity are those involving CuO_2 planes and that the possible mediators for electron pairing are spin (magnons) and lattice (phonons) excitations, besides (on top of) electron–electron interaction. Although the pairing seems to be dominated by spin fluctuations, the role of electron–phonon coupling in high T_c superconductivity cannot be disregarded. In particular, it has been theoretically suggested that a synergy between buckling phonon modes and magnetic excitations can lead to a considerable increase of T_c.[3,4]

The cuprate $CaCuO_2$ (CCO) with an infinite layer structure can be considered the most suitable compound for exploring the

nature of CuO_2 planes, because its structure is the simplest among the other parent compounds, consisting of an infinite stacking of square-type CuO_2 planes, separated by bare Ca ions.[5] This tetragonal phase of CCO, with a = b = 3.85 Å and c = 3.18 Å, can be stabilized in the form of thin films by using suitable substrates.[6] Moreover, among cuprates, the infinite-layer CCO is characterized by the strongest long-range magnetic interactions, as measured by resonant inelastic x-ray scattering on thin films.[7–9] For some aspects, however, CCO is an anomaly among cuprate parent compounds, because of the absence of apical oxygen for Cu in the CuO_2 planes, which makes hole doping almost impossible. The introduction of extra oxygen in the Ca plane is limited in CCO, and can reach a sufficient value for the appearance of superconductivity only at the interface with other oxides, like $SrTiO_3$, by the growth of heterostructures[10] or superlattices.[11,12]

Raman spectroscopy is a powerful tool for studying phonons and magnons in both superconducting and insulating cuprates. Although this technique has been fruitfully exploited in infinite layer cuprates,[12,13] refined, systematic Raman measurements have never been performed on high-quality single crystals of pure CCO films. According to factor group analysis, no Raman-active phonons are expected at the Γ point in the infinite layer structure (space group P 4/mmm) of CCO.[14] Nevertheless, a Raman spectrum has always been obtained in previous experiments, either due to a structural disorder induced by Sr substitution[15] or the introduction of oxygen in excess.[13] In both cases, a clear magnon-pair feature has also been observed for specific wavelength values of the incident radiation. This feature is well distinguishable from the phonon contributions in the Raman spectrum due to the large energy difference decoupling lattice- and spin-related degrees of freedom.

In this paper, we report an accurate study of the Raman spectrum of CCO films, with different extent of disorder, where both phonon and magnon-pair peaks are revealed. A disorder is introduced either by a strain induced by the substrate or by intercalating excess oxygen ions in the structure. We show that all the measured CCO crystals, under non-resonant conditions, do not exhibit any detectable Raman signal, in agreement with factor group analysis, confirming the high quality of the films. Under resonant conditions, inducing a disorder causes relaxation of the selection rules and the consequent appearance of a phonon spectrum.[16,17] Notably, even under resonant conditions, the film with the highest structural quality does not show any low-frequency Raman mode.

At odd with the phonon bands, a magnon-pair band is well visible in the Raman spectrum of all the samples studied, regardless of the origin and level of disorder. A systematic analysis of the trend of the magnon-pair intensity as a function of the polarization angle allows for the identification of two contributions to the spin-wave scattering mechanism: the first one, with representation B_{1g}, is dominant in intensity and substantially identical in the three samples, while the second one, much less intense, with representation A_{1g}, is enhanced in CCO-LAO, where the degree of disorder is maximum.

METHODS

Three CCO films were grown by pulsed-laser deposition (KrF excimer laser, λ = 248 nm) at a temperature around 600 °C, on different substrates and oxidizing conditions. The first sample, named CCO-LSAT hereafter, has been grown on a $[LaAlO_3]_{0.3}[Sr_2AlTaO_6]_{0.7}$ (LSAT) substrate, at an oxygen pressure of 10 Pa. The second sample, named CCO-LSAT-O_3 hereafter, has been grown on a LSAT substrate at a pressure of 80 Pa exerted by a mixture of oxygen and 12% ozone, to increase the amount of excess oxygen ions in the structure. The third film, named CCO-LAO hereafter, has been grown on a $LaAlO_3$ (LAO) substrate at an oxygen pressure of 10 Pa. The substrate holder was kept at a distance of 2.5 cm from the CCO target, which was prepared by a standard solid-state reaction.[10,11,18] All films have thicknesses between 30 and 40 nm.

All films were structurally characterized by Cu K_α x-ray Diffraction (XRD) measurements in a θ-2θ Bragg-Brentano geometry. In the inset of Fig. 1, the x-ray diffraction spectrum of the CCO-LSAT film is shown. The spectrum reveals that the film is single phase, with a c-axis parameter c = 3.19 Å. The high structural quality of this film, due to the very good match between the lattice parameters of CCO and LSAT substrates (a_{CCO} = 3.85 Å, a_{LSAT} = 3.87 Å), is confirmed by the very narrow rocking curve shown in Fig. 1 (black line), with FWHM = 0.07° and by visible finite size oscillations (not shown). In the same figure, we also show the rocking curves of the other two samples. It is evident that they are definitely larger than the first one, indicating the occurrence of a structural disorder. The lower structural quality of these films is partly reflected by the smaller intensity of the Bragg peaks, given the similar thickness and dimension of the three samples. For the CCO-LSAT-O_3 sample, in which the film is grown on the same LSAT substrate, the disorder is mainly due to the random introduction of extra oxygen ions in the structure, namely, in the Ca planes, where oxygen finds space to enter and sits in the apical position of the Cu atoms in the underlying CuO_2 plane.[10,13] The introduction

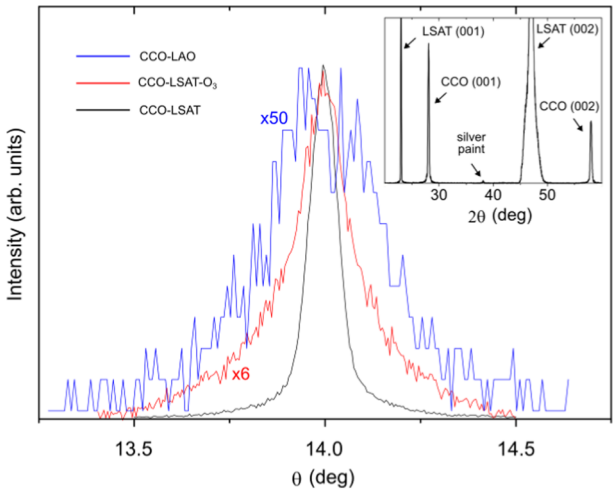

FIG. 1. Rocking curves (ω-scan) for the (001) diffraction peak of the three films CCO-LAO, CCO-LSAT, and CCO-LSAT-O_3. The full width at half maximum for the CCO-LSAT film is 0.07°, indicating a very small mosaic spread. Inset: $\theta - 2\theta$-scan for the clean CCO-LSAT sample.

of extra oxygens alters the stoichiometry of the system and produces a slight hole-doping of the CuO_2 planes. Indeed, the room temperature resistance of CCO-LSAT-O_3 is definitely lower than that of the other two samples. On the other hand, in CCO-LAO, the disorder is induced by the lattice mismatch between CCO and LAO ($a_{LAO} = 3.78$ Å), which leads to the growth of a strained CCO film. The strain in the film affects the structural (and in some cases, also physical) properties of the material. If the lattice misfit is large, as in the CCO-LAO film, crystal defects, such as dislocations and antiphase boundaries, are generally created to relieve the strain, even at small film thicknesses. In the case of compressive strain, as for the CCO-LAO film, out of plane distortions are expected, with enhancement of buckling of the otherwise almost flat CuO_2 and Ca planes. The critical thickness d_c, above which the strain is relieved, with the consequent nucleation of defects, can be roughly estimated by $d_c = \frac{a_s^2}{2}\frac{1}{|a_f - a_s|}$, where a_f and a_s are the film and the substrate in plane lattice parameters, respectively. In the CCO-LAO film, d_c = 10 nm, well below the actual film thickness (about 30–40 nm).

Raman spectra were collected with a Horiba LabRam HR Evolution microspectrometer coupled with a grating monochromator (with 600 lines/mm or 1800 lines/mm, corresponding to a spectral resolution of ∼3 and ∼1 cm^{-1}, respectively) and a charge coupled device detector. Two distinct lasers were employed as light sources, namely, a He–Ne laser at 633 nm (excitation energy $E_i = 1.96$ eV) and a solid state laser at 532 nm (E_i = 2.33 eV). The laser was focused on the sample surface through a 100x objective, resulting in a ∼1 μm spot size.

Polarization-dependent measurements were carried out, at 532 nm, rotating the sample by an angle θ about its vertical c-axis. The sample was oriented so that, for $\theta = 0°$, the a-axis of CCO was parallel to the polarization direction of the incident laser. An analyzer, placed before the monochromator, allowed for selecting the scattered radiation with a polarization direction either parallel (parallel configuration) or perpendicular (perpendicular configuration) to the incident one.[19] For further details, see the supplementary material.

EXPERIMENTAL RESULTS

CCO, whose structure belongs to the space group $P4/mmm$, possesses eight vibrational modes, among which two are acoustic, $A_{2u} + E_u$, five are infrared active, $2A_{2u} + 3E_{2u}$, and one is silent, B_{2u}.[14] In the ideal crystal, no active modes are, thus, expected in the Raman spectrum.

Figure 2 shows the Raman measurements carried out on CCO-LSAT, CCO-LSAT-O_3, and CCO-LAO in the 50–1400 cm^{-1} range. In all the three samples, the spectra collected with a 532 nm excitation wavelength (green lines in Fig. 2), according to the selection rules, exhibit no peaks but those belonging to the substrate, confirming the high crystalline quality of the CCO films synthesized. As we move to the 632 nm excitation laser, a whole new set of peaks appears in the three samples, indicating the occurrence of a resonance mechanism between the incident radiation and the charge-transfer (CT) gap at about 1.8 eV in the CCO band structure.[13,15,18]

The resonance contributions greatly vary in the three samples. While in CCO-LSAT only a few low-intensity bands appear above 1000 cm^{-1}, as shown in Figs. 2(a) and 2(b), the CCO-LSAT-O_3 film exhibits, additionally, some discernible contributions at ∼80 cm^{-1} and in the 150–300 cm^{-1} range [see Figs. 2(c) and 2(d)]. The resonant Raman activity is further enhanced in CCO-LAO, which displays four well-defined peaks below 300 cm^{-1} and a composite ensemble of intense features above 400 cm^{-1} [see Figs. 2(e) and 2(f) (red lines)], possibly associated with overtones and combination modes of low-energy Raman-inactive phonons.

A direct comparison between the Raman spectra of the samples collected at 633 nm and the XRD measurements, discussed in the Methods section, reveals that there exists a clear correlation between the degree of disorder in the crystal lattice, approximately evaluated by the width of the rocking curve in Fig. 1, and the resonant Raman signal. In the low-frequency region of the spectrum, taking the featureless CCO-LSAT spectrum as a reference, we see that the intercalation of excess oxygen in CCO-LSAT-O_3 weakly activates some broad bands, which evolve into intense and sharp peaks in the strained lattice of CCO-LAO.

Notably, the three peaks observed at ∼186, ∼235, and ∼296 cm^{-1} in CCO-LAO, shown in Fig. 2(e), seem to have an almost perfect correspondence with the infrared active modes reported in Refs. [14,20]. In particular, the two lowest-frequency modes are primarily due to vibrations involving Ca and Cu atoms along the c axis (A_u mode) and in the ab plane (doubly degenerate E_u), respectively, while the peak at ∼296 cm^{-1} can be ascribed to a vibrational buckling mode with E_u representation involving, mainly, the motion of O atoms along the c axis. As for the peak at 80 cm^{-1}, well discernible only in CCO-LAO, its assignation is more controversial. The peak frequency cannot be ascribed to any of the CCO phonons at the Γ point, nor to a combination of modes involving two of these phonons. The theoretical calculations of phonon dispersion[21,22] show that the frequency of this peak is comparable with that of a quadrupolar mode at the M point of the Brillouin zone, which is basically a plane buckling vibration involving displacements of the Ca atoms in the z-direction. Another possibility is that the peak is associated with Cu-O bond buckling modes, which were found to lie below 40 meV in $Nd_{1+x}Ba_{2-x}Cu_3O_{7-\delta}$ by resonant inelastic x-ray scattering (RIXS) measurements. In CCO, these modes, which might include the 80 cm^{-1} peak, could be activated when out-of-plane distortion (buckling) is present in the lattice due to the compressive strain in CCO-LAO, and appear in the spectrum under resonance conditions.

Differently from the resonant Raman spectrum below 1400 cm^{-1}, whose features greatly vary depending on the level of disorder, the spectral region above 2000 cm^{-1} shows a similar behavior in CCO-LSAT, CCO-LSAT-O_3, and CCO-LAO. In this range, the Raman spectrum of all the three CCO films displays a broad and asymmetric band centered at ∼3000 cm^{-1}, ascribable to a magnon-pair scattering process based on the previous measurements from the literature.[13,15] This feature is selectively activated in the samples when we excite with radiation at E_i = 2.33 eV (532 nm), while it is completely quenched as we move to the $E_i = 1.96$ eV (633 nm) laser, that is close to the CT gap of CCO (∼1.8 eV).[13,15,18]

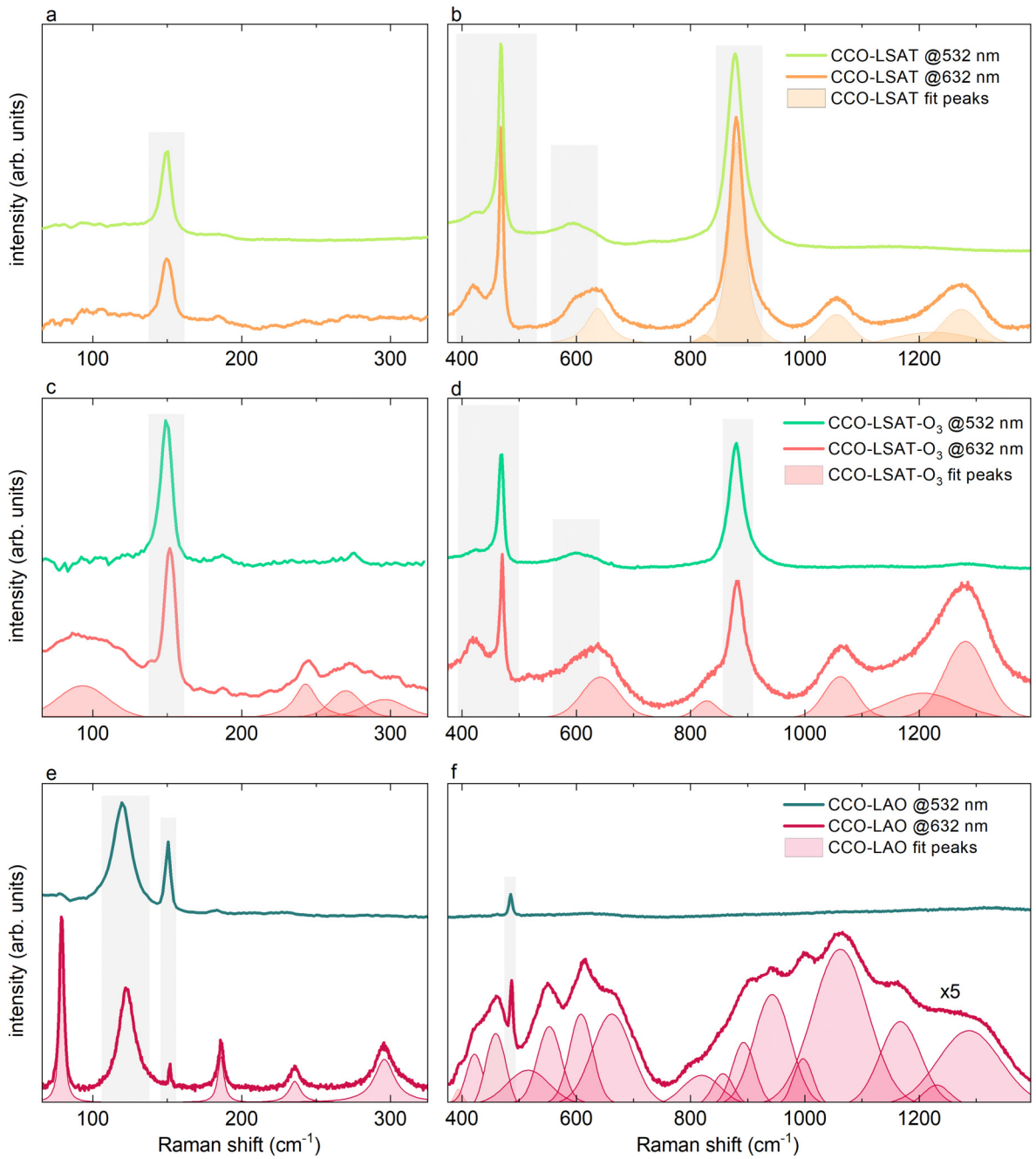

FIG. 2. (a) and (b) Raman spectrum of CCO-LSAT collected with a 532 nm (green line) and a 633 nm (red line) laser in the 50–400 cm^{-1} and 400–1400 cm^{-1} ranges, respectively. Each spectrum has been normalized to the intensity of the substrate peak at ∼150 cm^{-1}. The green spectrum in both (a) and (b) has been rigidly shifted upward for the sake of clarity. (c) and (d) Raman spectrum of CCO-LSAT-O_3 synthesized introducing excess oxygen ions in the structure collected with a 532 nm (green line) and a 633 nm (red line) laser in the 50–400 cm^{-1} and 400–1400 cm^{-1} ranges, respectively. Each spectrum has been normalized to the intensity of the substrate peak at ∼150 cm^{-1}. The green spectrum in both (c) and (d) has been rigidly shifted upward. (e) and (f) Raman spectrum of CCO-LAO collected with a 532 nm (green line) and a 633 nm (red line) laser in the 50–400 cm^{-1} and 400–1400 cm^{-1} ranges, respectively. Each spectrum has been normalized to the intensity of the substrate peak at ∼120 cm^{-1}. The green spectrum in both (e) and (f) has been rigidly shifted upward. The red spectrum in panel (f) has been multiplied by a factor 5 to better visualize the peaks. In all these panels, filled lines represent the fitting curve to the data, while the Raman peaks of the substrate (LAO or LSAT) have been marked with gray rectangles. Full Raman spectra of the bare substrates are shown in the supplementary material.

The suppression of the magnon-pair peak when the excitation energy is close to the CT gap, and the enhancement of it at higher E_i in cuprate parent compounds has been the subject of some debate in the past.[15,23–27]

In Ref. 27, Chubukov and Frenkel proposed a theory for the magnon-pair resonant Raman scattering based on the so-called *triple resonance*. This theory predicts a first resonance (i.e., an increase in the magnon-pair peak intensity) at excitation energy $E_{res_1} \simeq E_{CT} + 2.9J$, where E_{CT} is the charge transfer gap value and J is the nearest neighbor exchange interaction, and a second stronger resonance at higher excitation energies. On the other hand, no triple resonance conditions are predicted by this model for excitation energies around E_{CT}. Indeed, in our case, we do not see the magnon-pair peak for $E_i = 1.96$ eV, which is near E_{CT}, whereas we observe a clear peak for $E_i = 2.33$ eV (see Fig. 3), which is slightly above the predicted first resonance value $E_{res_1} \sim 1.8 + 3 \cdot 0.157 \sim 2.27$ eV, where we used $E_{CT} \sim 1.8$ eV[13,15,18] and $J \sim 0.157$ meV, as extracted from RIXS data.[7,8] Another possible explanation for the suppression of the magnon-pair peak at $E_i \sim E_{CT}$ might be given by the fact that, when CCO is excited at such E_i, a hole in the oxygen $2p$ state and an electron in the Cu $3d_{x^2-y^2}$ upper Hubbard state are created.[28] This event might produce ferromagnetic interaction between Cu spins and oxygen hole spins, known to suppress antiferromagnetic Cu spin order in superconducting (doped) cuprates. Moreover, the electrons created in the $3d_{x^2-y^2}$ upper Hubbard state reduce the (super)exchange interaction between the nearest

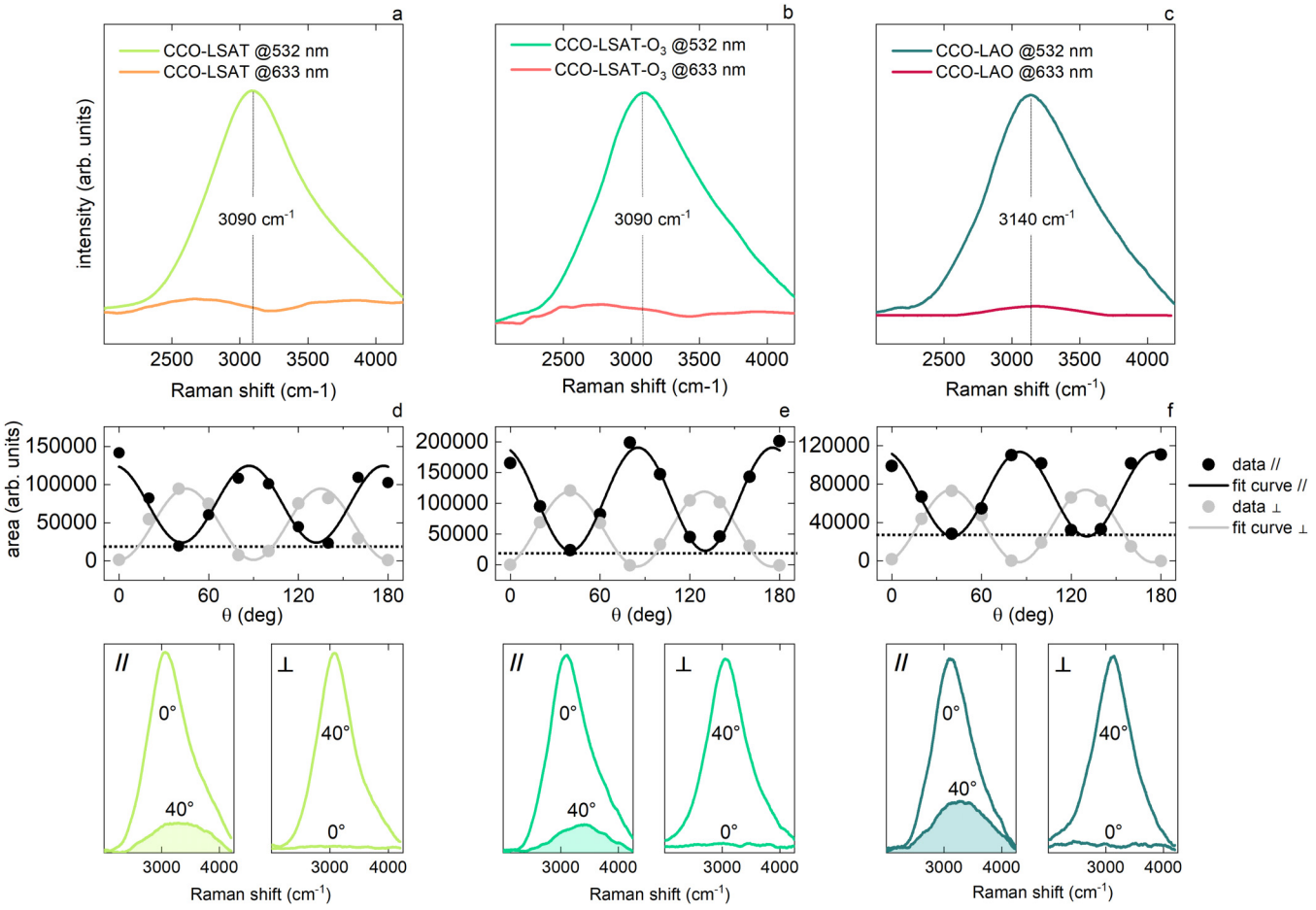

FIG. 3. (a)–(c) Raman spectra in the range 2000–4000 cm^{-1} collected with a 532 nm (green lines) and a 633 nm (red lines) laser for CCO-LSAT, CCO-LSAT-O_3, and CCO-LAO, respectively. Green spectra have been obtained as the average between the spectra measured on varying the polarization angle θ. In panels (a) and (b), red curves are obtained by subtracting the photoluminescence spectrum of the LSAT substrate to the spectrum collected on CCO-LSAT and CCO-LSAT-O_3, respectively (see the supplementary material). (d)–(f) Area of the magnon-pair peak (excited with the 532 nm laser) as a function of the polarization angle θ for CCO-LSAT, CCO_3-LSAT, and CCO-LAO, respectively. Black (gray) dots correspond to the values of the area obtained from the integral of the spectra in the parallel ($//$) (perpendicular ($\perp$)) configuration; the continuous black and gray lines represent the fitting curve $f(\theta) = constant + |c \cdot (\sin^2(\theta) - \cos^2(\theta))|^2$ and $g(\theta) = |2c \cdot \cos\theta \sin\theta|^2$, respectively. Lower panels show a comparison between the spectra at 0° and 40° for each sample in both parallel and perpendicular configurations.

neighbor Cu ions because of the presence of two electrons in the $3d$ state.[15]

In the Raman spectrum acquired at 2.33 eV, the magnon-pair band displays comparable widths in the three films and similar asymmetrical profiles. The peak energy, on the other hand, is shifted by nearly 50 cm^{-1} in CCO-LAO (3140 cm^{-1}) compared with the two samples grown on LSAT (3090 cm^{-1}).

In the framework of the antiferromagnetic spin 1/2 Hisenberg model, the energy position of the magnon-pair band E_{mp} in the Raman spectrum is related to the value of the nearest neighbor exchange interaction J: $E_{mp} \sim 2.7\,J$.[29,30] In our case, using $J \sim 157$ meV, estimated by fitting RIXS data using a simple nearest-neighbor Heisenberg model,[8] a magnon-pair band centered at ~424 meV ~ 3400 cm^{-1} is obtained. This value is higher than the experimental values obtained in the three samples: ~3140 cm^{-1} in CCO-LAO and ~3090 cm^{-1} in both CCO-LSAT-O_3 and CCO-LSAT films. The 2D AFM spin 1/2 Heisenberg model, therefore, fails in giving accurately the magnon-pair peak energy. This discrepancy could be well reconciled if we consider the role of the Higgs mode, associated with the amplitude oscillation of the magnetic order parameter, in the light scattering process from spin-waves.[31,32]

Indeed, theoretical calculations[31] suggested that the Higgs mode shows up in the dominant magnon-pair Raman response, mediating the magnon-magnon interactions and leading to a shift of the peak to lower energy $E_{mp} \sim 2.44\,J$, compared to the simple spin-wave analysis $E_{mp} \sim 2.7\,J$.

From this equation, we obtain $E_{mp} \simeq 3090\ cm^{-1}$, which is perfectly in line with the experimental result obtained for the CCO films grown on LSAT. The shift in energy observed in the CCO-LAO sample could be explained by the increase of disorder in the crystal due to the higher lattice mismatch with the substrate. Indeed, it was observed that, when momentum conservation is relaxed, due, for example, to the introduction of disorder in the system, as structural defects, the excitation process becomes more local, driving an increase in the peak energy.[33] Notably, this kind of disorder does not lead to a broadening of the peak,[33,34] as we can directly observe by comparing the spectra of the three films, where no substantial variation of the peak width is observed.

The proposed Higgs mode model[31,32] might also account for the broad and asymmetric line shape of the magnon-pair peak, typically observed in 2D AFM systems. Indeed, the Higgs mode is expected to show up in the Raman spectrum as an additional contribution centered at energies slightly higher than E_{mp}.[31,35] Other possible explanations for the asymmetric profile of the magnon-pair band include phonon-induced disorder by magnon-pair/phonon interaction,[34] finite magnon lifetime due to magnon-magnon scattering,[33] multi-magnon contributions, and higher-order (beyond next-neighbor) exchange terms.[36]

In other important cuprate parent compounds, such as LCO and YBCO, a bi-magnon Raman peak has been observed, with the same broad and asymmetric line shape as in CCO. In LCO, a Raman study as a function of temperature[37] reports that at room temperature, the bi-magnon peak is very similar to the one of CCO, with the presence of spectral weight at the high energy side of the peak. At low temperature, this spectral weight evolves in a pronounced shoulder, possibly connected to the Higgs mode.[31] On the other hand, in YBCO, no additional peak appears at low temperature.[35] For both the systems, by using the model which takes into account the presence of the Higgs mode in the Raman spectrum, the extracted value of J is very close to the one obtained by other techniques,[38,39] as it was shown for CCO in this work.

To investigate the composite nature of the magnon-pair band in our three samples, we analyzed the dependence of band intensity on varying the relative orientation between the crystal lattice and the polarization direction of the incident and the detected radiation.

As shown in Fig. 3, the intensity of the magnon-pair band measured at $E_i = 2.33$ eV possesses a clear sinusoidal trend as a function of the in-plane polarization angle θ.[40] The periodicity of this sinusoidal trend, equal to 90°, is compatible with that expected for an irreducible representation B_{1g}, which is commonly accepted as the dominant contribution to the magnon-pair excitation.[30,34]

By calculating the Raman intensity vs the polarization angle θ, using the appropriate form for the B_{1g} tensor in the space group $p4/mmm$ $\begin{pmatrix} c & 0 & 0 \\ 0 & -c & 0 \\ 0 & 0 & 0 \end{pmatrix}$, we obtain a function proportional to $|c \cdot (\cos^2\theta - \sin^2\theta)|^2$ in the parallel configuration and proportional to $|2c \cdot \cos\theta \sin\theta|^2$ in the perpendicular configuration. These two θ functions describe well the experimental trends measured in the two configurations, as shown in Figs. 3(d)–3(f).

Based on the calculated θ functions for B_{1g}, we would expect the magnon-pair intensity to vanish at the minima of the sinusoidal trend ($\theta = 45°, 135°$) in the parallel configuration. In the experimental data, however, a well distinguishable band is still observed around these θ values, indicating a possible contribution from the (low-intensity) A_{1g} representation; see lower panels in Fig. 3. In the classical theory, only B_{1g} scattering intensity is predicted for the planar nearest-neighbor Heisenberg antiferromagnet.[27] However, it has been demonstrated that accounting for quantum fluctuations in the ground state leads to additional allowed scattering in the A_{1g} and B_{2g} symmetries.[24,41] In the present case, the polarization dependence of the observed feature is coherent with the A_{1g} representation described by the diagonal tensor $\begin{pmatrix} a & 0 & 0 \\ 0 & a & 0 \\ 0 & 0 & b \end{pmatrix}$, which results in a contribution with constant intensity as a function of θ in the parallel configuration.

Looking at the relative intensity of the magnon-pair band at $\theta = 40°$ with respect to the band at $\theta = 0°$, $I_{40°}/I_{0°}$, in the parallel configuration, we notice that $I_{40°}/I_{0°}$ is equal to ~0.16 in both samples grown on LSAT, while it is more than doubled (~0.40) in CCO-LAO, indicating that the A_{1g} contribution tends to be enhanced by a strain-induced disorder (see lower panels in Fig. 3). In the perpendicular configuration, on the other hand, the intensity of the band at the minima of the sinusoidal trend ($\theta = 0°, 90°, 180°$) is zero in all the three samples, as shown in Figs. 3(d)–3(f). This observation further supports the assignment of this contribution to the A_{1g} representation, based on the simple calculations reported in the supplementary material.

Overall, we notice that the magnon-pair scattering process is more robust with respect to the increase in the degree of disorder

of the crystal lattice compared with the resonant phononic response. In particular, the strain-induced disorder in CCO-LAO drives some mild variations in the position and spectral composition of the band, while the intercalation of oxygen in excess in CCO-LSAT-O_3 seems to leave the magnon-pair response substantially unchanged, suggesting that low-level hole doping does not affect the spin excitation in CCO.

SUMMARY AND CONCLUSION

In this work, we carried out an extensive XRD and Raman investigation of epitaxial CCO films, in which different growth conditions were exploited to achieve a controlled modulation of the degree of disorder introduced in the crystal lattice.

The stoichiometric CCO film synthesized on a LSAT substrate proved itself as a nearly-ideal crystal, with significantly improved quality compared with the previous attempts reported in the literature, providing a reliable reference to account for the response of disorder-activated effects in defective samples. The latter was obtained either by intercalating oxygen in excess in the lattice, CCO-LSAT-O_3, resulting in a mild increase of disorder, or by growing the CCO film on a LAO substrate, CCO-LAO, with large lattice mismatch, which favored the formation of structural defects responsible for a much larger increase of disorder.

The results from Raman measurements showed that, under non-resonant conditions, the phonon spectrum of CCO in all the three samples displays no significant activity, according to the selection rules. As the energy of the exciting radiation nearly matches the value of the CT gap of CCO, resonant contributions appear in the phonon spectrum, whose number and intensity greatly vary depending on the growth conditions. A strong, direct correlation was observed between the degree of disorder in the crystal lattice and the enhancement of the resonant Raman activity with respect to the reference sample CCO-LSAT. This correspondence allows exploiting the phonon spectrum at resonance conditions as an optical benchmark complementary or, possibly, alternative to XRD, to evaluate the crystal quality in epitaxial CCO films.

Regarding the magnon-pair band around 3000 cm^{-1}, observable at 532 nm, well above the resonance with the CT gap, the overall profile was found to remain similar in the three samples, apart from a small shift of the peak energy in the CCO-LAO film.

The analysis of the magnon-pair peak energy and the line shape points toward the presence of a Higgs mode (oscillations of the amplitude of the magnetic order parameter), which contributes to the Raman spectrum of the infinite layer cuprate leading to a decrease in the magnon-pair peak energy and to its characteristic line shape.

Systematic measurements of the magnon-pair spectrum as a function of the polarization angle θ allowed us to extract a sinusoidal trend for the intensity compatible with the assignation of the magnon-pair band to the B_{1g} representation. The observation of a non-zero signal in the parallel configuration, at angles close to the minima of the sinusoidal trend, was interpreted as a sign of a secondary contribution with representation A_{1g}, whose intensity remains constant as a function of θ, due to the diagonal form of the corresponding tensor. Looking at the intensity ratio of the magnon-pair spectrum at $\theta = 40^\circ$ to that at $\theta = 0^\circ$, we noticed that the A_{1g} contribution is more than doubled in the film grown on LAO compared with the two films grown on LSAT, indicating a relationship between the enhancement of the A_{1g} signal and the degree of disorder in the CCO lattice.

In conclusion, our work offers an insight into the response of CCO epitaxial films to both strain- and doping-induced disorders exploring structural, lattice dynamic, and spin dynamic properties. Benchmark signatures of disorder-related mechanisms were identified in the XRD, phonon, and spin-wave spectra, providing a valuable reference for future research on CCO and other cuprate parent compounds. Overall, our results point to a larger sensitivity of phonon excitations to defects compared with magnon excitations, in the light scattering response from $CaCuO_2$ crystals, suggesting a decoupling between lattice- and spin-related degrees of freedom.

SUPPLEMENTARY MATERIAL

See the supplementary material for Raman spectra of the substrates and additional information about the polarization-dependent measurements.

ACKNOWLEDGMENTS

E.S. acknowledges funding from Project ECS 0000024 Rome Technopole,—CUP B83C22002820006, NRP Mission 4 Component 2 Investment 1.5, Funded by the European Union—NextGenerationEU. D.D.C. acknowledges support by the project PRIN2020 "QT-FLUO" ID 20207ZXT4Z of the Ministry for University and Research (MUR) of Italy.

AUTHOR DECLARATIONS

Conflict of Interest

The authors have no conflicts to disclose.

Author Contributions

E. Stellino: Conceptualization (equal); Data curation (lead); Formal analysis (lead); Investigation (lead); Writing – original draft (lead). **P. Postorino:** Conceptualization (equal); Supervision (equal); Writing – review & editing (lead). **S. Sanna:** Data curation (equal); Methodology (equal); Writing – review & editing (equal). **A. Tebano:** Data curation (equal); Methodology (equal); Writing – review & editing (equal). **D. Di Castro:** Conceptualization (lead); Data curation (equal); Formal analysis (equal); Investigation (lead); Supervision (lead); Writing – original draft (lead).

DATA AVAILABILITY

The data that support the findings of this study are available from the corresponding author upon reasonable request.

REFERENCES

[1]J. G. Bednorz and K. A. Müller, "Possible high T_c superconductivity in the Ba-La-Cu-O system," Z. Phys. B Condens. Matter **64**(2), 189–193 (1986).
[2]D. J. Scalapino, "The case for $d_{x^2-y^2}$ pairing in the cuprate superconductors," Phys. Rep. **250**(6), 329–365 (1995).
[3]L. Braicovich, M. Rossi, R. Fumagalli, Y. Peng, Y. Wang, R. Arpaia, D. Betto, G. M. De Luca, D. Di Castro, K. Kummer, M. Moretti Sala, M. Pagetti,

G. Balestrino, N. B. Brookes, M. Salluzzo, S. Johnston, J. van den Brink, and G. Ghiringhelli, "Determining the electron-phonon coupling in superconducting cuprates by resonant inelastic x-ray scattering: Methods and results on $Nd_{1+x}Ba_{2-x}Cu_3O_{7-\delta}$," Phys. Rev. Res. **2**(2), 023231 (2020).
[4]S. Johnston, F. Vernay, B. Moritz, Z.-X. Shen, N. Nagaosa, J. Zaanen, and T. P. Devereaux, "Systematic study of electron-phonon coupling to oxygen modes across the cuprates," Phys. Rev. B **82**, 064513 (2010).
[5]T. Siegrist, S. M. Zahurak, D. W. Murphy, and R. S. Roth, "The parent structure of the layered high-temperature superconductors," Nature **334**(6179), 231–232 (1988).
[6]G. Balestrino, R. Desfeux, S. Martellucci, A. Paoletti, G. Petrocelli, A. Tebano, B. Mercey, and M. Hervieu, "Growth of $CaCuO_2$ and Sr_x Ca_{1-x} CuO_2 epitaxial films on $NdGaO_3$ substrates by pulsed laser deposition," J. Mater. Chem. **5**(11), 1879–1883 (1995).
[7]L. Martinelli, D. Betto, K. Kummer, R. Arpaia, L. Braicovich, D. Di Castro, N. B. Brookes, M. Moretti Sala, and G. Ghiringhelli, "Fractional spin excitations in the infinite-layer cuprate $CaCuO_2$," Phys. Rev. X **12**, 021041 (2022).
[8]Y. Y. Peng, G. Dellea, M. Minola, M. Conni, A. Amorese, D. Di Castro, G. M. De Luca, K. Kummer, M. Salluzzo, X. Sun, X. J. Zhou, G. Balestrino, M. Le Tacon, B. Keimer, L. Braicovich, N. B. Brookes, and G. Ghiringhelli, "Influence of apical oxygen on the extent of in-plane exchange interaction in cuprate superconductors," Nat. Phys. **13**(12), 1201–1206 (2017).
[9]L. Braicovich, L. J. P. Ament, V. Bisogni, F. Forte, C. Aruta, G. Balestrino, N. B. Brookes, G. M. De Luca, P. G. Medaglia, F. Miletto Granozio, M. Radovic, M. Salluzzo, J. van den Brink, and G. Ghiringhelli, "Dispersion of magnetic excitations in the cuprate La_2CuO_4 and $CaCuO_2$ compounds measured using resonant X-ray scattering," Phys. Rev. Lett. **102**, 167401 (2009).
[10]D. Di Castro, C. Cantoni, F. Ridolfi, C. Aruta, A. Tebano, N. Yang, and G. Balestrino, "High-T_c superconductivity at the interface between the $CaCuO_2$ and $SrTiO_3$ insulating oxides," Phys. Rev. Lett. **115**, 147001 (2015).
[11]D. Di Castro, M. Salvato, A. Tebano, D. Innocenti, C. Aruta, W. Prellier, O. I. Lebedev, I. Ottaviani, N. B. Brookes, M. Minola, M. Moretti Sala, C. Mazzoli, P. G. Medaglia, G. Ghiringhelli, L. Braicovich, M. Cirillo, and G. Balestrino, "Occurrence of a high-temperature superconducting phase in $(CaCuO_2)_n/(SrTiO_3)_m$ superlattices," Phys. Rev. B **86**, 134524 (2012).
[12]D. Di Castro, S. Caramazza, D. Innocenti, G. Balestrino, C. Marini, P. Dore, and P. Postorino, "Raman spectroscopy study of the interface structure in $(CaCuO_2)_n/(SrTiO_3)_m$ superlattices," Appl. Phys. Lett. **103**(19), 191903 (2013).
[13]D. Kan, A. Yamanaka, T. Terashima, and M. Takano, "Preparation and optical properties of single-crystalline $CaCuO_2$ thin films with infinite layer structure," Physica C **412-414**, 298–302 (2004).
[14]G. Burns, M. K. Crawford, F. H. Dacol, E. M. McCarron, and T. M. Shaw, "Phonons in $CaCuO_2$," Phys. Rev. B **40**(10), 6717–6720 (1989).
[15]M. Yoshida, S. Tajima, N. Koshizuka, S. Tanaka, S. Uchida, and T. Itoh, "Two-magnon and two-phonon excitations in some parent insulating compounds of the high-T_c cuprates," Phys. Rev. B **46**(10), 6505–6510 (1992).
[16]S. Sotgiu, T. Venanzi, F. Macheda, E. Stellino, M. Ortolani, P. Postorino, and L. Baldassarre, "Raman scattering with infrared excitation resonant with the $MoSe_2$ indirect band gap," Phys. Rev. B **106**, 085204 (2022).
[17]L. Graziotto, F. Macheda, T. Venanzi, G. Marchese, S. Sotgiu, T. Ouaj, E. Stellino, C. Fasolato, P. Postorino, M. Metzelaars, P. Kögerler, B. Beschoten, M. Calandra, M. Ortolani, C. Stampfer, F. Mauri, and L. Baldassarre, "Infrared resonance raman of bilayer graphene: Signatures of massive fermions and band structure on the 2D peak," Nano Lett. **24**(6), 1867–1873 (2024).
[18]A. Perucchi, P. Di Pietro, S. Lupi, R. Sopracase, A. Tebano, G. Giovannetti, F. Petocchi, M. Capone, and D. Di Castro, "Electrodynamic properties of an artificial heterostructured superconducting cuprate," Phys. Rev. B **97**, 045114 (2018).
[19]I. Pallecchi, E. Stellino, P. Postorino, A. Iyo, H. Ogino, M. Affronte, and M. Putti, "Experimental investigation of electronic interactions in collapsed and uncollapsed $LaFe_2As_2$ phases," Phys. Rev. B **108**, 014512 (2023).
[20]B. K. Agrawal and S. Agrawal, "Structural, dynamical, and electronic properties of $CaCuO_2$," Phys. Rev. B **48**(9), 6451–6455 (1993).
[21]O. K. Andersen, S. Y. Savrasov, O. Jepsen, and A. I. Liechtenstein, "Out-of-plane instability and electron-phonon contribution tos- and*d*-wave pairing in high-temperature superconductors LDA linear-response calculation for doped $CaCuO_2$ and a generic tight-binding model," J. Low Temp. Phys. **105**(3-4), 285–304 (1996).
[22]S. Y. Savrasov and O. K. Andersen, "Linear-response calculation of the electron-phonon coupling in doped $CaCu_2$," Phys. Rev. Lett. **77**(21), 4430–4433 (1996).
[23]S. Sugai, "Phonon Raman scattering in $(La_{1-x}Sr_x)_2CuO_4$ single crystals," Phys. Rev. B **39**(7), 4306–4315 (1989).
[24]P. E. Sulewski, P. A. Fleury, K. B. Lyons, S.-W. Cheong, and Z. Fisk, "Light scattering from quantum spin fluctuations in R_2CuO_4 (R=La, Nd, Sm)," Phys. Rev. B **41**(1), 225–230 (1990).
[25]R. Liu, M. V. Klein, D. Salamon, S. L. Cooper, W. C. Lee, S.-W. Cheong, and D. M. Ginsberg, "Raman studies of charge-transfer insulating cuprates," J. Phys. Chem. Solids **54**(10), 1347–1350 (1993).
[26]M. Mayer, P. Knoll, M. Pressl, S. Lo, and E. Holzinger-Schweiger, "Two magnon resonance Raman scattering in doped $YBa_2Cu_3O_{6.3}$ single crystals," Phys. C **235-240**, 1097–1098 (1994).
[27]A. V. Chubukov and D. M. Frenkel, "Resonant two-magnon Raman scattering in antiferromagnetic insulators," Phys. Rev. Lett. **74**(15), 3057–3060 (1995).
[28]A. Fujimori, E. T. Muromachi, Y. Uchida, and B. Okai, "Spectroscopic evidence for strongly correlated electronic states in La-Sr-Cu and Y-Ba-Cu oxides," Phys. Rev. B **35**(16), 8814 (1987).
[29]K. B. Lyons, P. A. Fleury, L. F. Schneemeyer, and J. V. Waszczak, "Spin fluctuations and superconductivity in $Ba_2YCu_3O_{6+\delta}$," Phys. Rev. Lett. **60**(8), 732–735 (1988).
[30]G. Blumberg, P. Abbamonte, M. V. Klein, W. C. Lee, D. M. Ginsberg, L. L. Miller, and A. Zibold, "Resonant two-magnon Raman scattering in cuprate antiferromagnetic insulators," Phys. Rev. B **53**(18), R11930–R11933 (1996).
[31]S. A. Weidinger and W. Zwerger, "Higgs mode and magnon interactions in 2D quantum antiferromagnets from Raman scattering," Eur. Phys. J. B **88**(9), 237 (2015).
[32]D. Podolsky, A. Auerbach, and D. P. Arovas, "Visibility of the amplitude (Higgs) mode in condensed matter," Phys. Rev. B **84**, 174522 (2011).
[33]W. H. Weber and G. W. Ford, "Simple model for the linewidth of the two-magnon Raman feature observed in high T_c superconductors," Phys. Rev. B **40**(10), 6890–6895 (1989).
[34]F. Nori, R. Merlin, S. Haas, A. W. Sandvik, and E. Dagotto, "Magnetic Raman scattering in two-dimensional spin-1/2 Heisenberg antiferromagnets: Spectral shape anomaly and magnetostrictive effects," Phys. Rev. Lett. **75**(3), 553–556 (1995).
[35]L. Tassini, W. Prestel, A. Erb, M. Lambacher, and R. Hackl, "First-order-type effects in CuO_2 at the onset of superconductivity," Phys. Rev. B **78**, 020511 (2008).
[36]R. Coldea, S. M. Hayden, G. Aeppli, T. G. Perring, C. D. Frost, T. E. Mason, S.-W. Cheong, and Z. Fisk, "Spin waves and electronic interactions in La_2CuO_4," Phys. Rev. Lett. **86**(23), 5377–5380 (2001).
[37]B. Muschler, W. Prestel, L. Tassini, R. Hackl, M. Lambacher, A. Erb, S. Komiya, Y. Ando, D. C. Peets, W. N. Hardy, R. Liang, and D. A. Bonn, "Electron interactions and charge ordering in CuO_2 compounds," Eur. Phys. J. Spec. Top. **188**(1), 131–152 (2010).
[38]N. S. Headings, S. M. Hayden, R. Coldea, and T. G. Perring, "Anomalous high-energy spin excitations in the high-T_c superconductor-parent antiferromagnet La_2CuO_4," Phys. Rev. Lett. **105**(24), 247001 (2010).
[39]D. Reznik, P. Bourges, H. F. Fong, L. P. Regnault, J. Bossy, C. Vettier, D. L. Milius, I. A. Aksay, and B. Keimer, "Direct observation of optical magnons in $YBa_2Cu_3O_{6.2}$," Phys. Rev. B **53**(22), R14741–R14744 (1996).
[40]P. A. Fleury and S. P. S. Porto, "Light scattering by spin waves," J. Appl. Phys. **39**(2), 1035–1041 (1968).
[41]R. R. P. Singh, P. A. Fleury, K. B. Lyons, and P. E. Sulewski, "Quantitative determination of quantum fluctuations in the spin-$\frac{1}{2}$ planar antiferromagnet," Phys. Rev. Lett. **62**(23), 2736–2739 (1989).